Role of Alumina Coating on Li−Ni−Co−Mn−O Particles as Positive Electrode Material for Lithium-Ion Batteries

Seung-Taek Myung,[†,‡] Kentarou Izumi,[†] Shinichi Komaba,*[,†,||] Yang-Kook Sun,[§] Hitoshi Yashiro,[†] and Naoaki Kumagai[†]

Department of Frontier Materials and Functional Engineering, Graduate School of Engineering, Iwate University, 4-3-5 Ueda, Morioka, Iwate 020-8551, Japan, VK Corporation, 67 Jije-Dong, Pyongtaek-City, Kyonggi-Do 450−090, South Korea, and Department of Chemical Engineering, Hanyang University, Seungdong-Gu, Seoul 133-791, South Korea

Received March 14, 2005

The interface reaction between Al_2O_3-coated $Li[Li_{0.05}Ni_{0.4}Co_{0.15}Mn_{0.4}]O_2$ and liquid electrolyte was investigated. The Al_2O_3-coated $Li[Li_{0.05}Ni_{0.4}Co_{0.15}Mn_{0.4}]O_2$ showed no large difference in the bulk structure, comparing to bare $Li[Li_{0.05}Ni_{0.4}Co_{0.15}Mn_{0.4}]O_2$. The coated Al_2O_3 was found to have an amorphous structure from X-ray diffraction study. A small amount of Al_2O_3 coating (0.25 wt % in the final composition) showed that a uniform mesoporous Al_2O_3-coating layer whose thickness is of about 5 nm covers $Li[Li_{0.05}Ni_{0.4}Co_{0.15}Mn_{0.4}]O_2$ particles, as confirmed by transmission electron microscopy. At higher concentration (2.5 wt % in the final composition), the irregular tens of nanometer-sized Al_2O_3 powders were observed on the surface of the active material instead of the uniform coating layer. Despite the insulating nature of Al_2O_3, the thin coating was effective to improve the battery performances, depending on the thickness of the Al_2O_3-coating layer, and used electrolytic salt. The Al_2O_3 coating resulted in a higher capacity retention, especially at 60 °C. The alumina layer was significantly protective against HF attack into the electrolyte during cycling so that the decomposition of active material from HF attack would be greatly suppressed. The lower impedance would be ascribed to the positive effects on the electrode/electrolyte interface, the less amount of decomposition of active material by HF and/or scavenging of HF by Al_2O_3-coating layer into the electrolyte. These effects made it possible to maintain the morphology of active material during extensive cycling. Meanwhile, the bare particles were severely degraded by cycling due to HF.

Introduction

Recently, several kinds of 4 V class positive electrode materials are commercially available, that is, $LiCoO_2$, $LiNiO_2$, and $LiMn_2O_4$. Among them, Lithium cobalt oxide, $LiCoO_2$, is the most popular and practical positive electrode material in lithium secondary battery systems. This material has several advantages, ease of preparation, high electronic conductivity, high rechargeable capacity, good rate capability, and so forth.[1−3] Meanwhile, this material has a poor thermal stability relative to Mn-based and Fe-based materials.[4,5] Dissolution of Co element further accelerates the capacity fading of $LiCoO_2$.[6,7]

To maintain high capacity, there are two kinds of ways to improve the nature of active materials, partial substitution and coating of active materials. Modification of positive electrode material by substitution is greatly effective with respect to structural stabilization, good cyclability, and thermal stability even at a highly oxidized state. However, such substitutions were usually done for electrochemically active elements so that it, in turn, caused a lowering of capacity and Li^+ diffusion because the substituents are usually electrochemically inactive ingredients, that is, Al, Mg, Zn, and so on.[8−12] On the other hand, a coating approach is beneficial with respect to delivery of the original capacity because there is no reduction of the amount of electrochemically active element in the parent oxide. Therefore, improvements of electrochemical properties are possible to achieve by usage of a very small amount of coating of electrode materials.

Several reports have been made about metal oxide coating for lithiated transition metal oxide. Physical and electrochemical properties were significantly improved by Al_2O_3

* Corresponding author. Phone and Fax: +81-3-5228-8749. E-mail: komaba@rs.kagu.tus.ac.jp.
† Iwate University.
‡ VK Corporation.
§ Hanyang University.
|| Present address: 1-3 Kagurazaka, Shinjuku, Tokyo 162-8601, Department of Applied Chemistry, Tokyo University of Science, Japan.

(1) Mizushima, K.; Jones, P. C.; Wiseman, P. J.; Goodenough, J. B. *Mater. Res. Bull.* **1980**, *15*, 783.
(2) Reimers, J. N.; Dahn, J. R. *J. Electrochem. Soc.* **1992**, *139*, 2091.
(3) Choi, Y.-M.; Pyun, S.-I.; Moon, S.-I. *Solid State Ionics* **1996**, *89*, 43.
(4) Kim, J.-S.; Prakash, J.; Selman, J. R. *Electrochem. Solid-State Lett.* **2001**, *4*, A141.
(5) Jiang, J.; Dahn, J. R. *Electrochem. Commun.* **2004**, *6*, 39.
(6) Amatucci, G. G.; Tarascon, J. M.; Klein, L. C. *Solid State Ionics* **1996**, *83*, 167.
(7) Myung, S.-T.; Kumagai, N.; Komaba, S.; Chung, H.-T. *Solid State Ionics* **2001**, *139*, 47.
(8) Pouillerie, C.; Croguennec, L.; Biensan, Ph.; Willmann, P.; Delmas, C. *J. Electrochem. Soc.* **2000**, *147*, 2061.
(9) Song, D.; Ikuta, H.; Uchida, T.; Wakihara, M. *Solid State Ionics* **1999**, *117*, 151.
(10) Subramanian, V.; Fey, G. T.-K. *Solid State Ionics* **2002**, *148*, 351.
(11) Kang, S.-H.; Amine, K. *J. Power Sources* **2003**, *119−121*, 150.
(12) Levasseur, S.; Menetrier, M.; Delmas, C. *J. Power Sources* **2002**, *112*, 419.

10.1021/cm050566s CCC: $30.25
Published on Web 06/15/2005

and ZrO_2 coating as suggested by Cho et al.[13,14] The coating resulted in reduced Co dissolution during cycling, and it, subsequently, caused improved capacity and its retention. They further explained that the coating resulted in no structural change with zero-strain. Faster Li^+ diffusion and rate capability with good cyclability were also reported by Wakihara et al.[15,16] and Eftekhari.[17] Dahn's group also agreed with the high-capacity retention by coating.[18] However, they revealed that coating had no effect against structural change as studied by in-situ XRD,[18] which is a controversial result of Cho et al.[14] Sun et al.[19,20] used ZnO coating on $LiNi_{0.5}Mn_{1.5}O_4$ and found a greatly improved cycling behavior at 5 V due to the reduced reactivity of HF with the ZnO interface.

Recently, a new concept of materials, such as $Li[Ni_{1/3}Co_{1/3}Mn_{1/3}]O_2$ and $Li[Ni_{1/2}Mn_{1/2}]O_2$, was introduced by Ohzuku et al.[21,22] The chemistries of these materials are quite interesting. Different from $LiNiO_2$, whose average oxidation state of Ni is +3, the formal charges of Ni, Co, and Mn in $Li[Ni_{1/3}Co_{1/3}Mn_{1/3}]O_2$ or $Li[Ni_{1/2}Mn_{1/2}]O_2$ are +2, +3, and +4, respectively. In this case, the average oxidation state of Mn is tetravalent so that the electrochemically inactive tetravalent Mn provides significant structural stability during electrochemical cycling even at a high-voltage cutoff limit of 4.6 V. Due to the reduced amount of Co^{3+}, the thermal stability was greatly improved at a highly oxidized state, comparing to $LiCoO_2$.[23] However, $Li[Ni_{1/3}Co_{1/3}Mn_{1/3}]O_2$ is known to have unstable cycling performance, and its capacity fades gradually, especially when charged to a higher voltage (~4.5 V versus Li).[24] Comparing to $LiCoO_2$, Co-poor $Li[Ni_{1/3}Co_{1/3}Mn_{1/3}]O_2$ or $Li[Ni_{1/2}Mn_{1/2}]O_2$ composition had also relatively poor rate capability.

We successfully coated $Li[Li_{0.05}Ni_{0.4}Co_{0.15}Mn_{0.4}]O_2$ with Al_2O_3 using a wet chemical process. The material contains less amount of Co so that the material may have a somewhat poor rate capability, comparing to $Li[Ni_{1/3}Co_{1/3}Mn_{1/3}]O_2$. From the above review,[13−18] it is found that battery performances obviously enhanced, by metal oxide coating, for example, cyclability and rate capability. With help from Al_2O_3 coating, therefore, such poor characteristics are expected to be improved. However, a detailed reason is not clarified yet from the above review. In this paper, we would like to report the possible reason of improved battery performances by metal oxide coating of positive electrode material by means of Al_2O_3-coated $Li[Li_{0.05}Ni_{0.4}Co_{0.15}Mn_{0.4}]O_2$.

(13) Cho, J.; Kim, Y. J.; Park, B. *J. Electrochem. Soc.* **2001**, *148*, A1110.
(14) Cho, J.; Kim, Y. J.; Kim, T. J.; Park, B. *Angew. Chem., Int. Ed.* **2001**, *40*, 3367.
(15) Kim, S.-S.; Kadoma, Y.; Ikuta, H.; Uchimoto, Y.; Wakihara, M. *Electrochem. Solid-State Lett.* **2001**, *4*, A109.
(16) Kottegoda, I. R. M.; Kadoma, Y.; Ikuta, H.; Uchimoto, Y.; Wakihara, M. *Electrochem. Solid-State Lett*. **2002**, *5*, A275.
(17) Eftekhari, A. *J. Electrochem. Soc*. **2004**, *151*, A1456.
(18) Chen, Z.; Dahn, J. R. *Electrochem. Solid-State Lett.* **2002**, *5*, A213.
(19) Sun, Y.-K.; Lee, Y.-S.; Yoshio, M.; Amine, K. *Electrochem. Solid-State Lett.* **2002**, *5*, A99.
(20) Sun, Y.-K.; Yoon, C. S.; Oh, I.-H; *Electrochim. Acta* **2002**, *48*, 503.
(21) Ohzuku, T.; Makimura, Y. *Chem. Lett*. **2001**, *30*, 642.
(22) Ohzuku, T.; Makimura, Y. *Chem. Lett*. **2001**, *30*, 744.
(23) Myung, S.-T.; Kim, G.-H.; Sun, Y.-K. *Chem. Lett.* **2004**, *33*, 1388.
(24) Yoon, W.-S.; Balasubramanian, M.; Yang, X.-Q.; Fu, Z.; Fischer, D. A.; McBreen, J. *J. Electrochem. Soc.* **2004**, *151*, 246.

Experimental Section

To prepare Al_2O_3-coated $Li[Li_{0.05}Ni_{0.4}Co_{0.15}Mn_{0.4}]O_2$, aluminum triisopropoxide (Kanto) was first completely dissolved in ethanol at room temperature. The active material, $Li[Li_{0.05}Ni_{0.4}Co_{0.15}Mn_{0.4}]O_2$ (3 M), was slowly poured into the solution. The starting ratio of $Li[Li_{0.05}Ni_{0.4}Co_{0.15}Mn_{0.4}]O_2$ versus aluminum triisopropoxide was 99:1 in weight. Then, the solution containing the active material was constantly stirred at 80 °C for 2 days, accompanied by a slow evaporation of solvent. The solution-treated, as-received, and bare $Li[Li_{0.05}Ni_{0.4}Co_{0.15}Mn_{0.4}]O_2$ powders were fired at 400 °C in air for 5 h in air.

X-ray diffractometry (XRD, Rigaku Rint 2200) and transmission electron microscopy (TEM; 200 kV, Hitachi, H-800) were employed to characterize the prepared powders. XRD data were obtained at $2\theta = 10-80°$, with a step size of 0.03° and a count time of 5 s. X-ray photoelectron spectroscopy (XPS, PHI 5600, Perkin-Elmer) measurements were performed to get information on the surface of Al_2O_3-coated $Li[Li_{0.05}Ni_{0.4}Co_{0.15}Mn_{0.4}]O_2$. Macro-mode (about 3 mm × 3 mm) Ar-ion etching was used to examine concentration depth profiles of the coated powders. The etching rate was estimated as 5 Å min^{-1} for silica.

For fabrication of positive electrodes, the prepared powders were mixed with carbon black and polyvinylidene fluoride (94:3:3) in *N*-methylpyrrolidinon. The slurry thus obtained was coated onto Al foil and roll-pressed at 120 °C in air. The electrodes were dried at 120 °C overnight in a vacuum state prior to use. Preliminary cell tests were done using 2016 coin-type cell adopting Li metal as the negative electrode. The long cycle-life tests were performed in laminated type full cell wrapped with Al pouch (thickness, 18 mm; width, 90 mm; and length, 160 mm). MCMB (Osaka gas) was used as the negative electrode. The electrolyte solution used was 1 M $LiPF_6$ in ethylene carbonate−diethyl carbonate (1:2 in volume). A preliminary cell formation was performed for Li-ion cell: five cycles were performed at room temperature at 0.01 ~ 0.5 *C* rates in the voltage range of 3.0 − 4.2 V. The *C*-rate is defined as the exchange of 0.5 F per formula unit in 1 h. The cells were charged and discharged between 3 and 4.2 V by applying constant current densities at 25 and 60 °C. *Ac*-impedance measurements using beaker type 3-electrode cell were carried out by applying 100 kHz to 1 mHz frequency range with an *ac*-amplitude of 10 mV_{rms} (HZ-3000, Hokuto Denko). The electrochemical cell was composed by the composite electrode as the working electrode, Li ribbon as the counter electrode, and Li needle as the reference electrode.

For HF titration, the cycled cells (adapting carbon as the negative electrode) were carefully disassembled and all contents of the cell washed thoroughly with Li salt-free solvent for one week in the glovebox. NaOH aqueous solution (Kanto) and Bromothymol Blue (BTB, Aldrich) as an indicating solution were used for the titration of the extensively cycled electrolyte.

To confirm the presence of byproducts on the surface of the active materials after extensive cycling, the cycled active materials were examined using a time-of-flight−secondary ion mass spectroscopy (ToF−SIMS, ULVAC-PHI TFS2000, Perkin-Elmer) surface analyzer operated at 10^{-9} Torr, equipped with a liquid Ga ion source and pulse electron flooding. During the analysis, the targets were bombarded by the 10 keV Ga beams with pulsed primary ion current varying from 0.3 to 0.5 pA. The total collection time was 300 s and rastered over a 12 mm × 12 mm area.

Results and Discussion

Figure 1 shows XRD patterns of bare and solution-treated $Li[Li_{0.05}Ni_{0.4}Co_{0.15}Mn_{0.4}]O_2$ fired at 400 °C for 5 h in air.

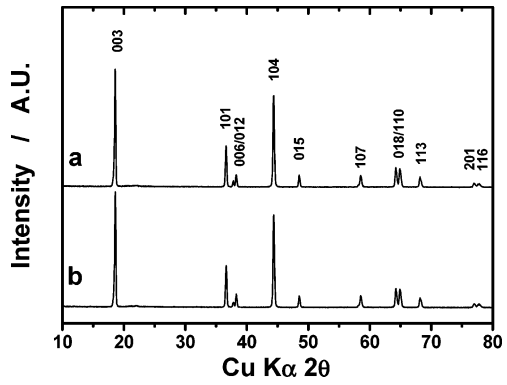

Figure 1. XRD patterns of (a) bare and (b) Al_2O_3-coated $Li[Li_{0.05}Ni_{0.4}Co_{0.15}Mn_{0.4}]O_2$ (0.25 wt %).

Table 1. Comparison of Lattice Parameters of Bare and Al_2O_3-Coated $Li[Li_{0.05}Ni_{0.4}Co_{0.15}Mn_{0.4}]O_2$ (0.25 wt %)[a]

$Li[Li_{0.05}Ni_{0.4}Co_{0.15}Mn_{0.4}]O_2$	*a*/Å	*c*/Å
bare	2.871(5)	14.273(25)
Al_2O_3-coated	2.871(3)	14.279(26)

[a]For comparison, the bare materials were also fired at 400 °C for 5 h in air.

The diffraction patterns can be identified as a hexagonal α-$NaFeO_2$ structure with space group $R\bar{3}m$ for bare and Al_2O_3-coated materials in Figure 1a,b, respectively. Though the $Li[Li_{0.05}Ni_{0.4}Co_{0.15}Mn_{0.4}]O_2$ was coated by foreign aluminum, there is no significant difference in the crystal structure after the coating, as seen in Figure 1 and Table 1, suggesting that Al doping did not occur in the parent oxide because the coated amount is very small in the final product (∼0.25 wt %) and/or the coating material is in an amorphous state when it is fired at the temperature as low as 400 °C. In fact, the *a*-axis parameter corresponds to the distance of metal and oxygen. If the distance is changed, it clearly means that foreign element should be incorporated into the crystal structure. Therefore, we believe that the coating layer consisted of amorphous Al_2O_3 in consideration of the starting material and the heat-treatment condition.

Figure 2 illustrates bright-field TEM images for the bare and Al_2O_3-coated $Li[Li_{0.05}Ni_{0.4}Co_{0.15}Mn_{0.4}]O_2$ varying the Al_2O_3-coating concentration. The bare material showed very smooth edge lines, and there is no other layer on the surface in Figure 2a. As can be seen in Figure 2b, the Al_2O_3-coated material (0.25 wt %) clearly showed a smooth and uniform coating line on the surface of $Li[Li_{0.05}Ni_{0.4}Co_{0.15}Mn_{0.4}]O_2$. When the coating layer was magnified, it exhibited a thin coating layer of about 5 nm in thickness and the coating layer could be a porous structure comparing to the active material in Figure 2c. With increasing coating amount to 2.5 wt %, the uniform layer is hardly distinguishable. The mesoporous coating structure was changed to nanoparticles whose particle size is of about 20−40 nm at the higher concentration of coating solution as shown in Figure 2d. Therefore, it is found that low concentration of Al_2O_3 resulted in a thin and uniform Al_2O_3-coating layer, but higher amount of Al_2O_3 coating led to nanosized Al_2O_3 particles on the surface of $Li[Li_{0.05}Ni_{0.4}Co_{0.15}Mn_{0.4}]O_2$.

Figure 3 presents STEM and EDX elemental mapping images of the Al_2O_3-coated $Li[Li_{0.05}Ni_{0.4}Co_{0.15}Mn_{0.4}]O_2$ powders (0.25 wt %). Al_2O_3 is homogeneously covered on the

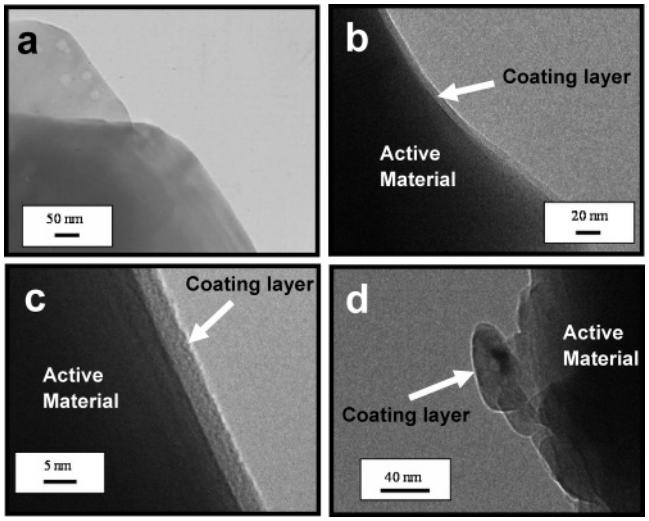

Figure 2. TEM bright-field images of (a) bare and Al_2O_3-coated $Li[Li_{0.05}Ni_{0.4}Co_{0.15}Mn_{0.4}]O_2$ (b−d): (b) 0.25 wt % of Al_2O_3-coated (at lower magnification), (c) 0.25 wt % of Al_2O_3-coated (at higher magnification), and (d) 2.5 wt % of Al_2O_3-coated $Li[Li_{0.05}Ni_{0.4}Co_{0.15}Mn_{0.4}]O_2$.

surface of $Li[Li_{0.05}Ni_{0.4}Co_{0.15}Mn_{0.4}]O_2$, which confirms the uniformity of Al_2O_3 coating shown in Figure 2b,c. The observed particle size of the active material was of about 1 μm in diameter. Clearly, Ni, Co, and Mn were well-distributed throughout the crystalline oxide.

XPS results further support the evidence of the uniform coating of $Li[Li_{0.05}Ni_{0.4}Co_{0.15}Mn_{0.4}]O_2$ by Al_2O_3 in Figure 4. At the beginning, the atomic concentration for Al element was of about 7%,as seen in Figure 4b. With increasing sputtering time, the relative intensities of Ni_{2p}, Mn_{2p}, and Co_{2p} became stronger as compared to their initial state in Figure 4a. On the other hand, that of the Al_{2s} was getting lower on sputtering. The concentration became gradually lower on Ar-ion etching, and it finally reached zero when the etching was done for 10 min in Figure 4b. Meanwhile, the concentration of Ni, Co, and Mn ingredients were getting higher after sputtering. Therefore, it is believed that the Al_2O_3-coating layer exists almost on the surface of $Li[Li_{0.05}Ni_{0.4}Co_{0.15}Mn_{0.4}]O_2$ powders.

Figure 5 exhibits continuous charge and discharge curves of the bare and Al_2O_3-coated $Li[Li_{0.05}Ni_{0.4}Co_{0.15}Mn_{0.4}]O_2$/Li cells by applying different current densities at 25 °C (1 C = 150 mA g^{-1}) between 3.3 and 4.3 V versus Li. The coated concentration of Al_2O_3 was 0.25 wt %. The cells were charged galvanostatically with 0.2 *C*, and then discharged at different *C*-rates. Obviously, the Al_2O_3-coated sample delivered a little higher capacity at all currents, comparing to bare material in Figure 5a. The similar results were also previously reported by Cho et al.,[13,14] Wakihara et al.,[15,16] and Eftekhari.[17] It seems from Figure 5 that Al_2O_3 coating was effective at achieving higher rate capability with respect to the delivered capacity.

Dependence of Al_2O_3 coating amount on the electrochemical properties of $Li[Li_{0.05}Ni_{0.4}Co_{0.15}Mn_{0.4}]O_2$/Li was examined and was shown in Figure 6. The cells were cycled at different *C*-rates at 25 °C. All cells had high-capacity and good-capacity retention even at high rates, as seen in Figure 6. The obtained capacity was greatly dependent on the coating

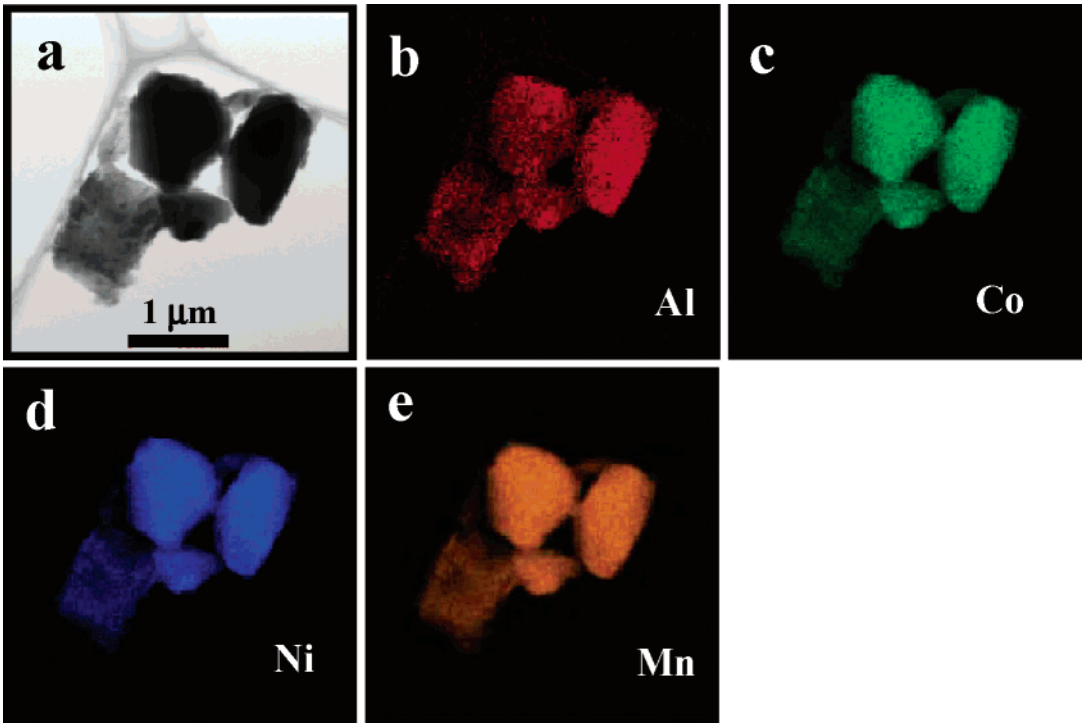

Figure 3. (a) STEM image and corresponding EDX elemental mappings of (b) Al, (c) Co, (d) Ni, and (e) Mn for the 0.25 wt % of Al_2O_3-coated $Li[Li_{0.05}Ni_{0.4}Co_{0.15}Mn_{0.4}]O_2$.

concentration of Al_2O_3, as expected. As the coating concentration becomes higher, the obtained capacity decreases due to the thicker Al_2O_3 insulating layer, as nanosized Al_2O_3 particles were observed in Figure 2d.

After reproducible rate capability tests during 12 cycles, the bare and Al_2O_3-coated $Li[Li_{0.05}Ni_{0.4}Co_{0.15}Mn_{0.4}]O_2$/Li cells were continuously cycled by applying different *C*-rates at 25 °C. The corresponding results appear in Figure 7. The bare material cycled at 1 *C* had a slow capacity fading in Figure 7a, and the capacity loss was of about 20 mAh g^{-1} during cycling (86.4% capacity retention). For the Al_2O_3-coated $Li[Li_{0.05}Ni_{0.4}Co_{0.15}Mn_{0.4}]O_2$ (1 *C* cycling) in Figure 7b, the cell showed superior cyclability and the capacity loss was only about 5 mAh g^{-1} during cycling (96.8% capacity retention). At 3 *C* cycling (Al_2O_3-coated) shown in Figure 8c, it delivered quite a higher capacity and the capacity loss was about 10 mAh g^{-1} showing 92.9% of capacity retention during cycling.

To observe long-term cycling properties, carbon electrode was employed as the negative electrode. Figure 8 exhibits initial discharge curves of the bare and Al_2O_3-coated $Li[Li_{0.05}Ni_{0.4}Co_{0.15}Mn_{0.4}]O_2$/C cells by applying different current densities at 25 and 60 °C between 3.0 and 4.2 V. At 1 *C*, the obtained discharge capacity was slightly smaller for the bare as compared to the Al_2O_3-coated $Li[Li_{0.05}Ni_{0.4}Co_{0.15}Mn_{0.4}]O_2$/C cell in Figure 8a. The voltage profiles were exactly matched for each other, which can say that the Al_2O_3-coating layer exists only on the surface of $Li[Li_{0.05}Ni_{0.4}Co_{0.15}Mn_{0.4}]O_2$ powders. If a small amount of Al_2O_3 is incorporated into the host structure, the corresponding voltage should vary as we previously reported in spinel $LiMn_{2-x}Al_xO_4$ [25] and $LiCo_{1-x}Al_xO_2$ systems.[7] This result confirms again that the coating media exists only on the surface of $Li[Li_{0.05}Ni_{0.4}Co_{0.15}Mn_{0.4}]O_2$. At 3 and 5 *C* rates, on the other hand, about 15−20% of the initial capacity decaying is observed for the bare sample, comparing to the Al_2O_3-coated $Li[Li_{0.05}Ni_{0.4}Co_{0.15}Mn_{0.4}]O_2$ in Figure 8b,c. Moreover, the difference in the operation voltage is found to be lower, about 0.1 V at 50% of depth of discharge (3 and 5 *C* rates). The cyclability for the bare and coated material was relatively good at room-temperature cycling in Figure 8a. At elevated temperature test (1 *C* rate at 60 °C), the Al_2O_3-coated material had somewhat higher capacity and operating voltage, comparing to the bare sample in Figure 8d. These results clearly indicate that the uniform coating of the surface of $Li[Li_{0.05}Ni_{0.4}Co_{0.15}Mn_{0.4}]O_2$ by Al_2O_3 led to higher capacity and lower resistance at various conditions. Capacity fading at 60 °C was about 34% at the 300th cycle for the bare material. Meanwhile, the fading was approximately 16% for the coated material in Figure 9b. From the above half- and full-cell results, it is found that the Al_2O_3 coating of $Li[Li_{0.05}Ni_{0.4}Co_{0.15}Mn_{0.4}]O_2$ is very effective at enhancing battery performances with respect to *C*-rate, capacity retention, and temperature properties.

To elucidate the difference in electrochemical properties, it was first doubted that the Al_2O_3 coating of active material may suppress the structural changes in the host structure as it was suggested by Cho et al.[14] Therefore, in-situ XRD measurements were carried out to understand structural changes of the bare and the Al_2O_3-coated $Li[Li_{0.05}Ni_{0.4}Co_{0.15}Mn_{0.4}]O_2$ materials. Diffraction peaks of stainless ex-met (revealed as S) are used as the internal standard. As Li^+ deintercalated from the host structure, (00*l*) peaks were gradually shifted toward lower angle for the bare and coated materials in Figure 10a,b, respectively. On the other hand,

(25) Myung, S.-T.; Komaba, S.; Kumagai, N. *J. Electrochem. Soc.* **2001**, *148*, A482.

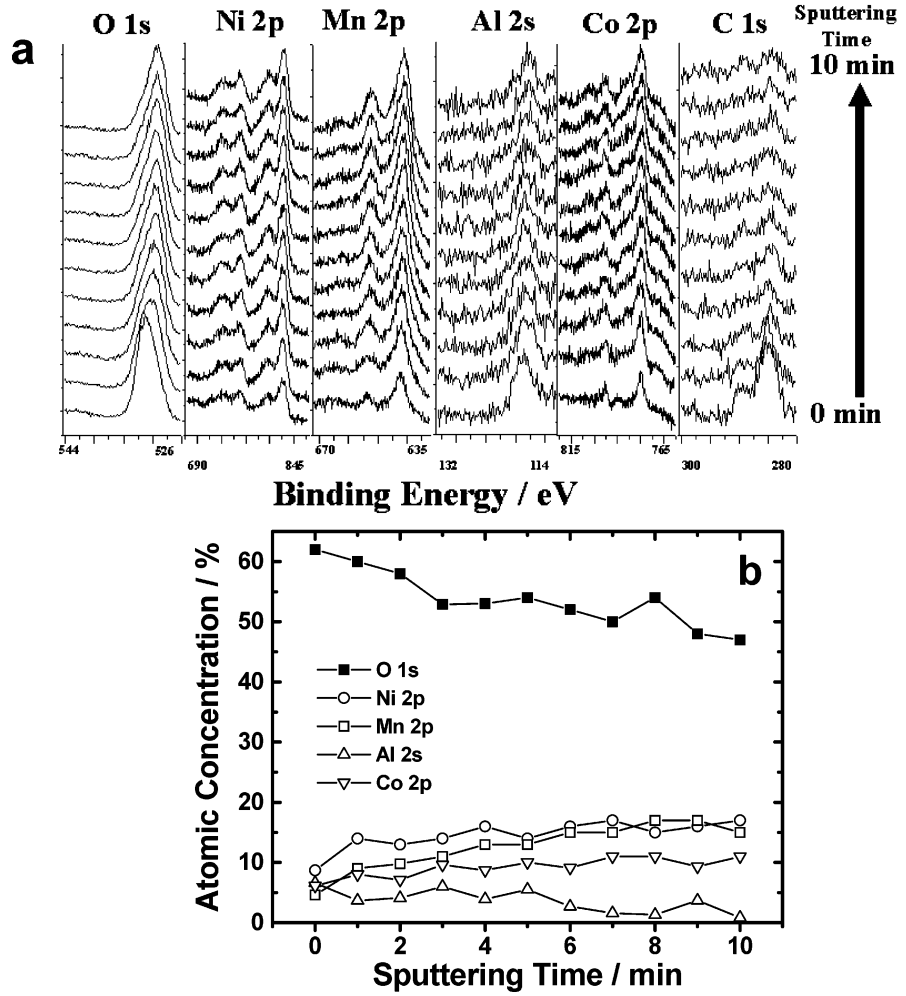

Figure 4. (a) XPS spectra for O, Ni, Mn, Al, Co, and C and (b) corresponding depth profile for the 0.25 wt % of Al_2O_3-coated $Li[Li_{0.05}Ni_{0.4}Co_{0.15}Mn_{0.4}]O_2$.

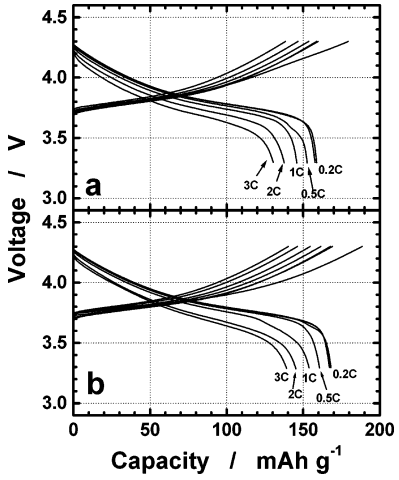

Figure 5. Rate capability of (a) bare and (b) 0.25 wt % of Al_2O_3-coated $Li[Li_{0.05}Ni_{0.4}Co_{0.15}Mn_{0.4}]O_2$/Li cells at 25 °C.

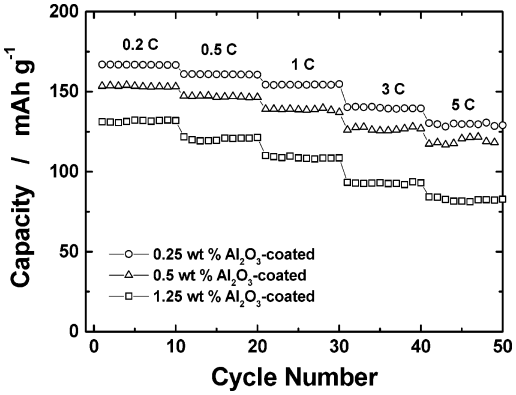

Figure 6. Rate capability and cyclability of Al_2O_3-coated $Li[Li_{0.05}Ni_{0.4}Co_{0.15}Mn_{0.4}]O_2$/Li cells at 25 °C with varying Al_2O_3 contents.

all other peaks were shifted smoothly toward a higher angle in 2θ during the first charge without any peaks of secondary phases in the XRD pattern of Figure 10a,b, which means that a single phase reaction occurred topotactically during Li^+ deintercalation. Apparently, there is no large difference in the XRD patterns for the bare and Al_2O_3-coated $Li[Li_{0.05}Ni_{0.4}Co_{0.15}Mn_{0.4}]O_2$ materials.

From in-situ XRD patterns in Figure 10, lattice parameters were calculated by a least-squares method and the results were shown in Figure 11. As Li^+ ions were extracted from the host structure, the *a*-axis decreased monotonically, which corresponds to the reduction of the metal−metal interslab distance, because the ionic radii of Ni^{3+}, Ni^{4+}, and Co^{4+}, formed during charge, are smaller than those of Ni^{2+} and Co^{3+}, respectively. This, therefore, leads to a decrease of metal−oxygen distance. The *c*-axis constant increased in the following deintercalation for $Li_{1-\delta}[Li_{0.05}Ni_{0.4}Co_{0.15}Mn_{0.4}]O_2$. The increase in the *c*-axis parameter is due to the increase in the Coulombic (electrostatic) repulsion force between the oxygen−oxygen layers by the ionicity of M−O bonding. Whether the active material is coated or not, suppression of

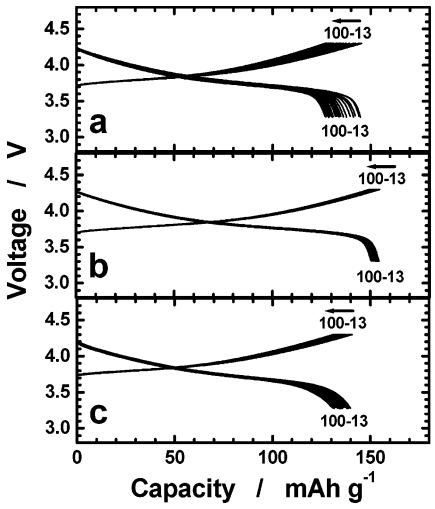

Figure 7. Continuous charge and discharge curves of $Li[Li_{0.05}Ni_{0.4}Co_{0.15}Mn_{0.4}]O_2$/Li cells at 25 °C: (a) bare at 1 *C*, (b) Al_2O_3-coated (0.25 wt %) at 1 *C*, and (c) Al_2O_3-coated (0.25 wt %) at 3 *C*. The cyclings were done after rate tests for 12 cycles.

the structural changes by Al_2O_3 coating was hardly observed from the in-situ XRD study, which is quite different from the report of Cho et al.[14] This would be because the coating amount of Al_2O_3 is quite small and the layer is composed of amorphous structure. From this result, it is believed that Al_2O_3 coating of active material does not contribute to the suppression of the structural changes during cycling in our experiment.

Hence, it was thought that the difference in battery performances would be related to the interface reaction including lithium intercalation/deintercalation at the interface between positive electrode and electrolyte. To provide more information for the improved electrochemical property, ac-impedance measurements were performed for the bare and Al_2O_3-coated $Li[Li_{0.05}Ni_{0.4}Co_{0.15}Mn_{0.4}]O_2$ during the first Li^+ deintercalation as a function of Li contents. Corresponding impedance spectra were presented as Cole−Cole plots in Figure 12. After fabrication of the electrochemical cell, the cell was aged for 2 days to reach equilibrium state at the electrode/electrolyte interface.

As shown in Figure 12, one can see a great difference in interface impedance. By comparing the diameter of the main semicircles, the charge-transfer resistance (R_{ct}) for the bare material was about two times larger than that for Al_2O_3-coated material, as described in Table 2. As Li^+ deintercalated from the host structure, the R_{ct} increases greatly for the bare $Li_{1-\delta}[Li_{0.05}Ni_{0.4}Co_{0.15}Mn_{0.4}]O_2$ in Figure 12a. On the other hand, sa mall increase is observed for the Al_2O_3-coated $Li_{1-\delta}[Li_{0.05}Ni_{0.4}Co_{0.15}Mn_{0.4}]O_2$ in Figure 12b. As mentioned in Table 2, the increase of R_{ct} for the bare material is almost twice of its initial R_{ct}. It is quite interesting to note that the thin Al_2O_3 layer, which covers the active material shown in Figure 2a−c, obviously enhanced the kinetics of the lithium intercalation in Figures 6−9, whereas Al_2O_3 is an electric insulator. If the coating layer is insulating, the layer should block the direct interconnections between active particles and an electrolyte solution, and this would deteriorate the charge transfer from active particles to the current collector, causing an increase in R_{ct}. However, the obtained results are quite different from this general expectation in Figures 7−9 and Table 2. Therefore, it is reasonable to think that the improved battery performances of the Al_2O_3-coated $Li[Li_{0.05}Ni_{0.4}Co_{0.15}Mn_{0.4}]O_2$ shown in Figures 7 and 9 would be related with the lower impedance of the coated active material which might depend on the thickness of the alumina layer.

Resistances (at 1 kHz) of the bare and Al_2O_3-coated $Li[Li_{0.05}Ni_{0.4}Co_{0.15}Mn_{0.4}]O_2$/C cells were also measured before and after cycling at 25 °C (5 *C*) and 60 °C (1 *C*), as described in Table 3. Obviously, the Al_2O_3-coated $Li[Li_{0.05}Ni_{0.4}Co_{0.15}Mn_{0.4}]O_2$/C cells showed greatly reduced resistance after cycling, especially cycling at 60 °C. The difference in resistance of cycling at 60 °C was about 20 times. This result clearly indicates that decomposition of active material or electrolyte was significantly suppressed by Al_2O_3 coating of active material.

The cycled cells were carefully disassembled, and all contents were washed thoroughly with Li salt-free solvent for one week in the glovebox. Figure 13 shows naked-eye images of separators selected from the extensively cycled

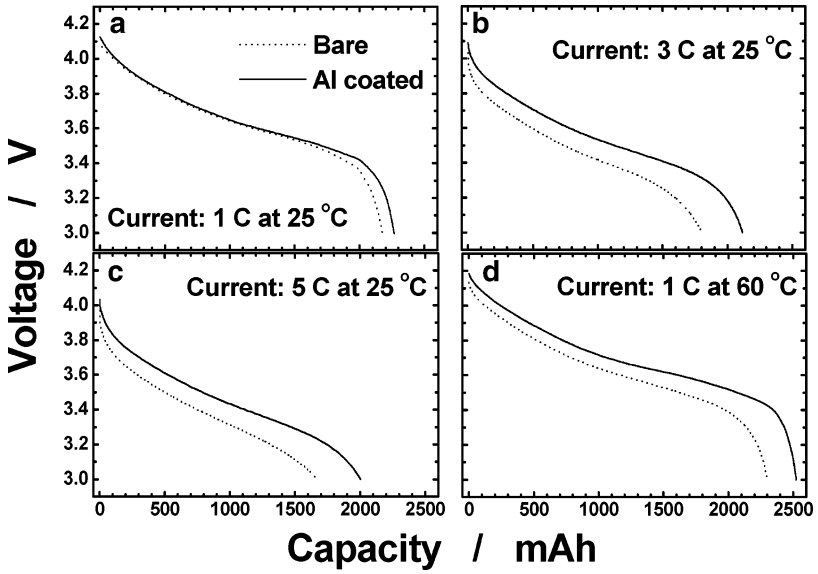

Figure 8. Initial discharge curves of bare and Al_2O_3-coated (0.25 wt %) $Li[Li_{0.05}Ni_{0.4}Co_{0.15}Mn_{0.4}]O_2$/C cells at 25 and 60 °C.

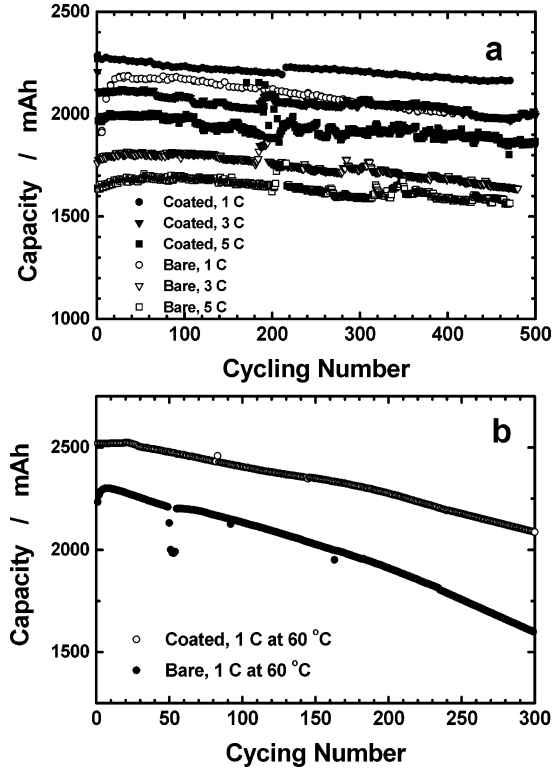

Figure 9. Cyclability of bare and Al_2O_3-coated (0.25 wt %) $Li[Li_{0.05}Ni_{0.4}Co_{0.15}Mn_{0.4}]O_2$/C cells at (a) 25 and (b) 60 °C.

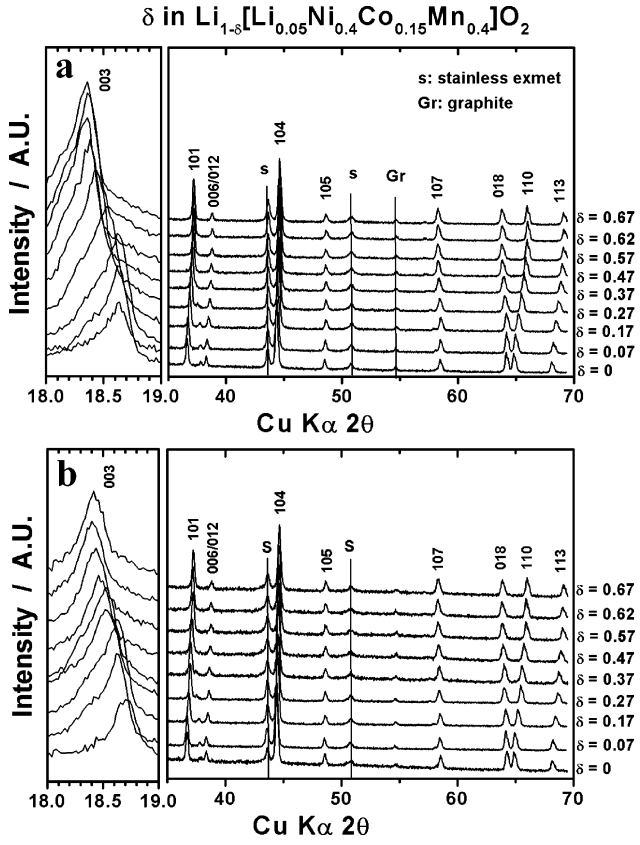

Figure 10. In-situ XRD patterns of (a) bare and (b) Al_2O_3-coated $Li[Li_{0.05}Ni_{0.4}Co_{0.15}Mn_{0.4}]O_2$ electrodes. Measurements were done during the first charge by applying 30 mA g^{-1} current. S designates stainless exmet, and Gr means graphite.

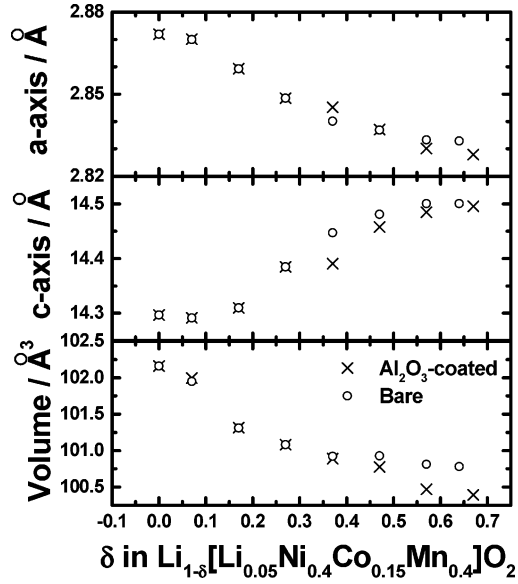

Figure 11. Variation in lattice parameters for bare and Al_2O_3-coated $Li_{1-\delta}[Li_{0.05}Ni_{0.4}Co_{0.15}Mn_{0.4}]O_2$. The lattice constants were calculated from the in-situ XRD pattern in Figure 10.

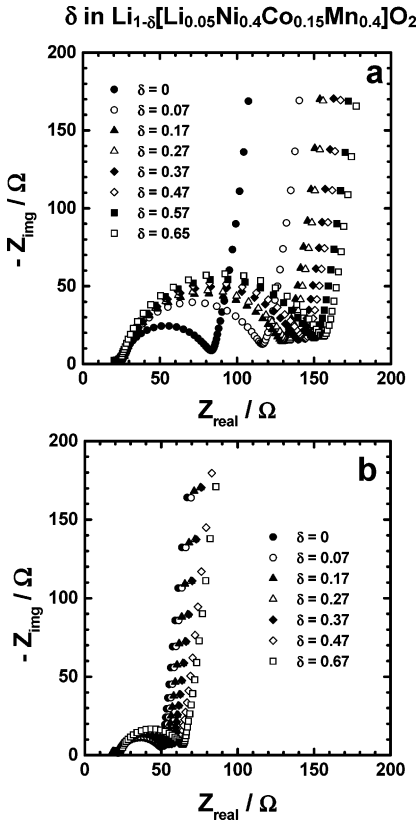

Figure 12. Cole−Cole plots of (a) bare and (b) Al_2O_3-coated $Li_{1-\delta}[Li_{0.05}Ni_{0.4}Co_{0.15}Mn_{0.4}]O_2$ during the first charge.

cells at 60 °C. One can see in Figure 13a that dark olive-green-colored compounds cover most of the separator. One the other hand, a relatively small area is covered by the compounds for the case of the separator of Al_2O_3-coated $Li[Li_{0.05}Ni_{0.4}Co_{0.15}Mn_{0.4}]O_2$/C cell in Figure 13b. Such compounds consisted of Ni, Co, and Mn elements that would be formed from the decomposition of active materials. The highest possibility for decomposition of the active material is due to HF attack in the electrolyte during cycling, because the propagation of HF is much facilitated at elevated temperature, such as 60 °C. Therefore, appropriate amounts

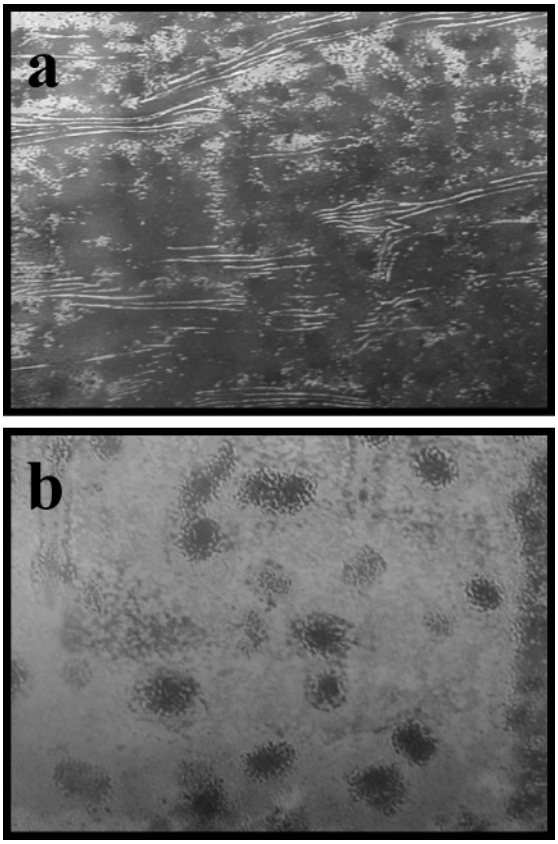

Figure 13. Separator images of (a) bare and (b) Al_2O_3-coated $Li[Li_{0.05}Ni_{0.4}Co_{0.15}Mn_{0.4}]O_2$/C cells after extensive cycling at 60 °C.

Table 2. Charge Transfer Resistances of Bare and Al_2O_3-Coated $Li_{1-\delta}[Li_{0.05}Ni_{0.4}Co_{0.05}Mn_{0.4}]O_2$ Calculated from Figure 13

δ in $Li_{1-\delta}[Li_{0.05}Ni_{0.4}Co_{0.05}Mn_{0.4}]O_2$	charge-transfer resistance (Ω)	
	bare	Al_2O_3-coated
$\delta = 0$	61.5	30.6
$\delta = 0.07$	94.7	32.7
$\delta = 0.17$	107.7	35.1
$\delta = 0.27$	111.6	37.4
$\delta = 0.37$	117.6	38.6
$\delta = 0.47$	121.9	43
$\delta = 0.57$	128	-
$\delta = 0.67$	135.4	44.4

Table 3. Comparison of Resistance at 1 kHz for Bare and Al_2O_3-Coated $Li[Li_{0.05}Ni_{0.4}Co_{0.15}Mn_{0.4}]O_2$/C Cells before and after Cycling at 25 and 60 °C

$Li[Li_{0.05}Ni_{0.4}Co_{0.15}Mn_{0.4}]O_2$/C cell	bare (mΩ)	Al_2O_3-coated (mΩ)
before cycle	6.83	6.12
after 500 cycles at 5 *C* (25 °C)	12.7	7.2
after 300 cycles at 1 *C* (60 °C)	780	36

of the washed solvent containing cycled electrolyte were analyzed by HF titration. The amount of HF was about 300 ppm for the bare material and 160 ppm for the Al_2O_3-coated $Li[Li_{0.05}Ni_{0.4}Co_{0.15}Mn_{0.4}]O_2$ as seen in Table 4 which had excellent battery performances in Figures 7 and 9. This result clearly means that propagation of HF is greatly suppressed by the Al_2O_3 coating during cycling so that the Al_2O_3-coated $Li[Li_{0.05}Ni_{0.4}Co_{0.15}Mn_{0.4}]O_2$/C cell was able to maintain the initial capacity of about 84%, whereas that of the bare was only 66% during 300 cycles at 60 °C. Consequently, it resulted in quite less of an increase in resistance after extensive cycling, especially 60 °C, leading to superior cyclability.

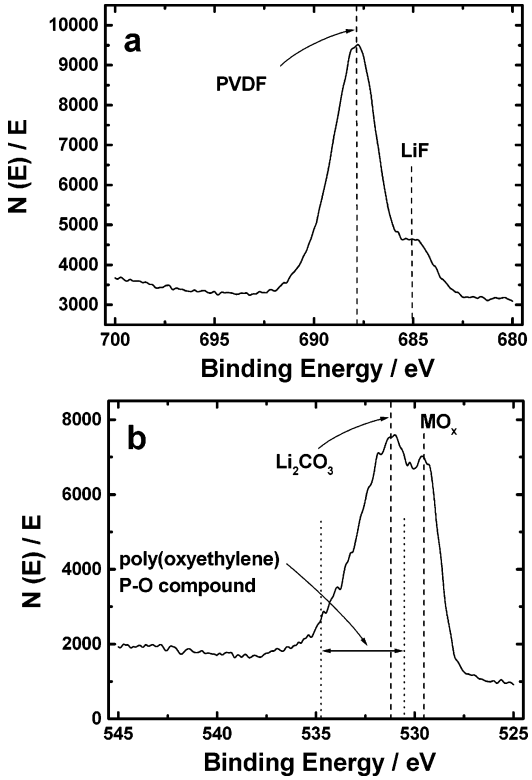

Figure 14. XPS spectra of the extensively cycled Al_2O_3-coated $Li[Li_{0.05}Ni_{0.4}Co_{0.15}Mn_{0.4}]O_2$ electrode at 60 °C: (a) F and (b) O spectra.

Table 4. Acidic Titration (as HF) Results Using Cycled Electrolyte for Bare and Al_2O_3-Coated $Li[Li_{0.05}Ni_{0.4}Co_{0.15}Mn_{0.4}]O_2$/C Cells after Extensive Cycling at 60 °C

$Li[Li_{0.05}Ni_{0.4}Co_{0.15}Mn_{0.4}]O_2$/C cell	acid content as HF (ppm)
bare	300
Al_2O_3-coated	163

From the above results in Figure 13 and Table 3, it was thought that the generated HF continuously attacks the active material in the electrolyte, and the active material, thus, consequently, decomposes as the cycle goes by, causing capacity fading as shown in Figures 7 and 9. Decomposition of $LiPF_6$ salt into the electrolyte was clearly seen by XPS observation of the extensively cycled Al_2O_3-coated $Li[Li_{0.05}Ni_{0.4}Co_{0.15}Mn_{0.4}]O_2$ electrode in Figure 14, and according to the following reactions, as suggested by Aurbach et al.[26] and Edström et al.:[27]

$$LiPF_6 \rightarrow LiF\downarrow + PF_5 \quad (1)$$

$$PF_5 + H_2O \rightarrow POF_3 + 2HF \quad (2)$$

$$POF_3 + 3Li_2O^- \rightarrow 6LiF\downarrow + P_2O_5\downarrow \text{ (or } Li_xPOF_y) \quad (3)$$

As seen in Figure 14 a, LiF was deposited on the surface of the active material. In Figure 14b, O_{1s} spectrum has a sharp feature around 529 eV originating from the oxygen of Al_2O_3-coated $Li[Li_{0.05}Ni_{0.4}Co_{0.15}Mn_{0.4}]O_2$. Another strong band occuring around 531−536 eV is due to both organic and inorganic material, typically poly(oxyethylene), P−O compound, and Li_2CO_3, which would be originated from solvent decomposition or contamination with air during sampling.

(26) Aurbach, D. *J. Electrochem. Soc.* **1989**, *136*, 906.
(27) Edström, K.; Gustafsson, T.; Thomas, J. O. *Electrochim. Acta* **2004**, *50*, 379.

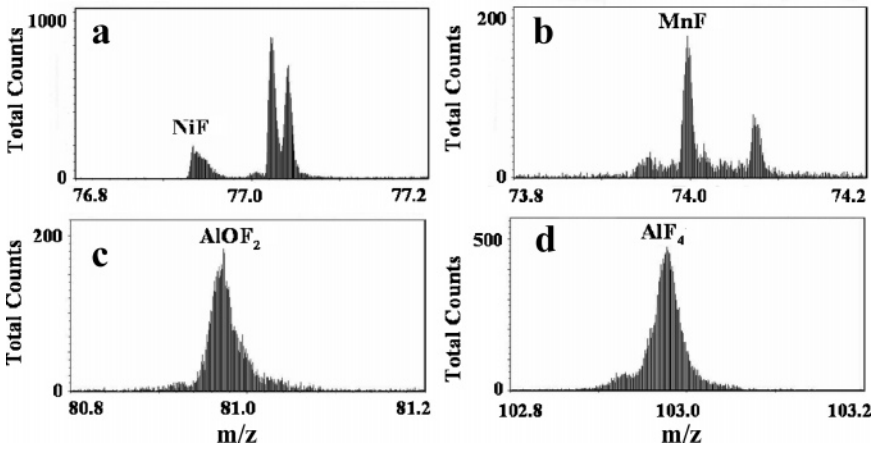

Figure 15. ToF−SIMS results (high mass resolution spectra) of extensively cycled Al_2O_3-coated $Li[Li_{0.05}Ni_{0.4}Co_{0.15}Mn_{0.4}]O_2$ electrode at 60 °C.

It is also obvious that if decomposition of the active material by the HF attack proceeds, byproduct is inevitably formed. To confirm the formed byproduct, ToF−SIMS observation was carried out for the Al_2O_3-coated $Li[Li_{0.05}Ni_{0.4}Co_{0.15}Mn_{0.4}]O_2$ electrode after extensive cycling at 60 °C, and the corresponding results were presented in Figure 15. Though quantitative analysis is difficult by ToF−SIMS, this tool has a very high sensitivity to detect molecule ions qualitatively for surface analysis. In fact, $LiPF_6$-based electrolyte always contains a small amount of water. The water amount is greatly propagated from the decomposition of $LiPF_6$ salt at elevated temperature. The existence of a small amount of water consequently causes breakdown of the electrolyte accompanying by HF generation. The generated HF attacks the Al_2O_3-coated $Li[Li_{0.05}Ni_{0.4}Co_{0.15}Mn_{0.4}]O_2$ particles; hence, it is possible to suppose that Ni, Co, and Mn ingredients produce byproducts on the surface of the active material by HF attack during extensive cycling. Then, the byproducts would be detected as fragments having Ni−F and Mn−F bonding as seen in Figure 15a,b, assuming the following reactions;

$$Li[Li_{0.05}Ni_{0.4}Co_{0.15}Mn_{0.4}]O_2 + 2HF + Li^+ + e^- \rightarrow Li_{1-\delta}[Li_{0.05}Ni_{0.4}Co_{0.15}Mn_{0.4}]O_2 + LiF + H_2O \quad (4)$$

$$MnO + 2HF \rightarrow MnF_2 + H_2O \quad (5)$$

$$CoO + 2HF \rightarrow CoF_2 + H_2O \quad (6)$$

$$NiO + 2HF \rightarrow NiF_2 + H_2O \quad (7)$$

Thus, these byproducts would adhere to the surface of the separator as shown in Figure 13, leading to great increase in resistance (Table 3). This decomposition would much easily occur for the case of bare $Li[Li_{0.05}Ni_{0.4}Co_{0.15}Mn_{0.4}]O_2$ because the material is directly exposed to HF. On the other hand, the Al_2O_3 layer covers the surface of $Li[Li_{0.05}Ni_{0.4}Co_{0.15}Mn_{0.4}]O_2$ so that such decomposition reactions would be delayed because the insulating Al_2O_3 layer works as a protecting layer against HF attack.

Moreover, Van Landschoot et al.[28] suggested that the Al_2O_3-coating layer scavenges the acidic HF species from the electrolyte. From their supposition, the following reaction was first considered: $Al_2O_3 + 6HF \rightarrow 2AlF_3 + 3H_2O$. However, the reaction did not occur directly. Surprisingly, ToF−SIMS gave us very interesting results because Al−O−F and Al−F fragments were detected as presented in Figure 15c,d. It is thought that the formation of Al−O−F would be in an intermediate stage to be transformed to Al−F bond which scavenges F^- from HF, assuming the following reactions based on ToF−SIMS results:

$$Al_2O_3 + 2HF \rightarrow Al_2O_2F_2 + H_2O \quad (8)$$

$$Al_2O_2F_2 + 2HF \rightarrow Al_2OF_4 + H_2O \quad (9)$$

$$Al_2OF_4 + 2HF \rightarrow 2AlF_3 + H_2O \quad (10)$$

From this reason, it is believed that the amount of HF generated during cycling is quite suppressed by the Al_2O_3 coating of $Li[Li_{0.05}Ni_{0.4}Co_{0.15}Mn_{0.4}]O_2$ with the interface effect as mentioned above.

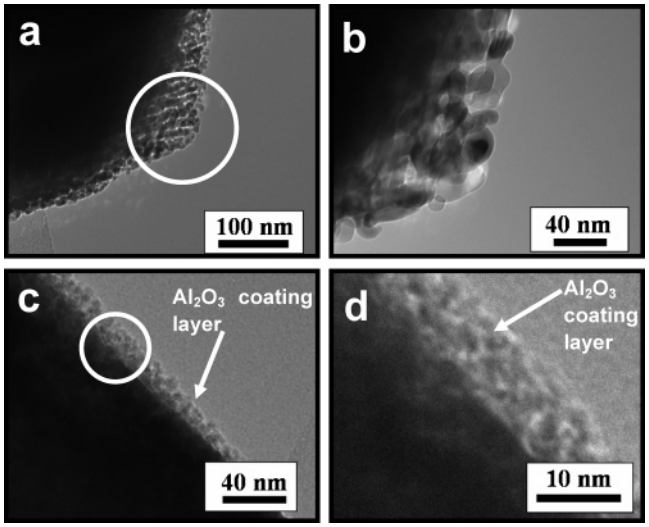

Figure 16. TEM bright-field images of extensively cycled bare and Al_2O_3-coated $Li[Li_{0.05}Ni_{0.4}Co_{0.15}Mn_{0.4}]O_2$ electrodes at 60 °C. Bare electrode, (a) lower magnification and (b) higher magnification. Al_2O_3-coated electrode, (c) lower magnification and (d) higher magnification.

Figure 16 exhibits TEM bright-field images of the extensively cycled bare and Al_2O_3-coated $Li[Li_{0.05}Ni_{0.4}Co_{0.15}Mn_{0.4}]O_2$. For the case of bare material which showed

(28) Van Landschoot, N.; Kelder, E. M.; Kooyman, P. J.; Kwakernaak, C.; Schoonman, J. *J. Power Sources* **2004**, *138*, 262.

relatively severe capacity fading at 60 °C, the material was severely damaged by electrochemical cycling as shown in Figure 16a. A magnified image clearly presents that the single particle was disrupted to smaller particle of which the particle size is about 20 nm in diameter in Figure 16b, comparing to Figure 2a. As mentioned above, such break-up of particles would be mainly ascribed to the HF attack into electrolyte during cycling. Moreover, the destroyed particles would lose the electric contact between active material and conducting agent so that the capacity fading and increase of polarization would be significantly facilitated during cycling as it was seen in Figures 8 and 9b for the bare material, especially cycling at 60 °C. The coating layer swelled a little after extensive cycling in Figure 16c,d, probably due to penetration of the electrolyte into the porous Al_2O_3-coating layer during the cycling. Also, it is clear from Figure 16c,d that the Al_2O_3-coated $Li[Li_{0.05}Ni_{0.4}Co_{0.15}Mn_{0.4}]O_2$ still maintained its original smooth edge by the Al_2O_3 coating, leading to relatively higher capacity retention in Figures 7 and 9 due to the Al_2O_3-coating layer working as protection and scavenging layer against HF attack into the electrolyte.

Such improved battery performances, especially at higher rates, usually appeared in inorganic material-coated systems, for example, Al_2O_3- and ZrO_2-coated graphite by Wakihara's group[15,16] and Al_2O_3-coated $LiCoO_2$ [13] and $LiCoPO_4$.[17] Summarizing the above results, it was found that the Al_2O_3-coated $Li[Li_{0.05}Ni_{0.4}Co_{0.15}Mn_{0.4}]O_2$ had greatly improved cyclability with high rechargeable capacity due to the impact of the Al_2O_3 coating in protecting the surface against HF attack in $LiPF_6$-containing electrolyte solution. And, the amphoteric surface of the Al_2O_3 layer scavenges the acidic HF species from the electrolyte. Van Landschoot et al.[28] experimentally proved that bulk electronic conductivity of the palletized Al_2O_3-coated $LiCo_{0.94}Fe_{0.06}VO_4$ is slightly higher than that of the bare. Furthermore, direct tunneling of electrons through the coating is also possible when the coating is thinner than 4 nm as described by Groner et al.[29] Generally, a relatively thick passive layer of Al_2O_3 is formed onto Al foil in air, but electrical contact on Al is easy through the insulating Al_2O_3 layer. From these considerations, higher capacity at 3 and 5 *C* is understandable for the Al_2O_3-coated $Li[Li_{0.05}Ni_{0.4}Co_{0.15}Mn_{0.4}]O_2$ as shown in Figures 8 and 9a; that is, the sufficiently thin Al_2O_3 layer does not interfere with the electrochemical reaction, and simultaneously, it would have the positive effects on the interface including solid electrolyte interface, electric double layer, and so on.

Conclusion

We have tried to understand the enhanced battery performances of Al_2O_3-coated $Li[Li_{0.05}Ni_{0.4}Co_{0.15}Mn_{0.4}]O_2$ as positive electrode material for lithium-ion battery. A uniform and thin Al_2O_3-coating layer was formed on the surface of $Li[Li_{0.05}Ni_{0.4}Co_{0.15}Mn_{0.4}]O_2$, and the layer (~5 nm) was composed of amorphous structure. Higher amount of Al_2O_3 coating produced tens of nanometer-sized Al_2O_3 particles on the surface of $Li[Li_{0.05}Ni_{0.4}Co_{0.15}Mn_{0.4}]O_2$. From TEM, STEM, and XPS analyses, it was found that the thin layer existed only on the surface of $Li[Li_{0.05}Ni_{0.4}Co_{0.15}Mn_{0.4}]O_2$ particles. The Al_2O_3-coated $Li[Li_{0.05}Ni_{0.4}Co_{0.15}Mn_{0.4}]O_2$ had much higher capacity when the coating layer was thinner employing $LiPF_6$-containing electrolyte. The coating was obviously effective at higher rates and elevated temperature battery performances with help of the thin, insulating Al_2O_3 layer, which significantly suppressed the propagation of HF during extensive cycling. The reduced generation of HF consequently resulted in less decomposition of the active material so that the impedance of the cell was quite lower comparing with employing the bare $Li[Li_{0.05}Ni_{0.4}Co_{0.15}Mn_{0.4}]O_2$ electrode. Furthermore, the coating layer worked as an HF scavenger, as confirmed by ToF−SIMS. These combinations, simultaneously, made it possible to maintain the original particle shape of the Al_2O_3-coated $Li[Li_{0.05}Ni_{0.4}Co_{0.15}Mn_{0.4}]O_2$ powders during cycling at long terms. From the above results, it was found that the thickness of the coating layer and the uniformity are critical conditions to have better battery performances. Therefore, it is concluded that the thin coating layer does not disturb the Li^+ intercalation reaction at the interface between electrode and electrolytic interface, and it substantially improves battery performances.

Acknowledgment. The authors thank Mr. S. Takahashi and Ms. A. Ueyama for their helpful assistance in the experimental work. This study was financially supported by the program in 2000−2004 "Development of Rechargeable Lithium Battery with High Energy/Power Density for Vehicle Power Sources" of the Industrial Technology Research Grant Program from the New Energy and Industrial Technology Development Organization (NEDO), Japan.

CM050566S

(29) Groner, M. D.; Elam, J. W.; Fabreguette, F. H.; George, S. M. *Thin Solid Films* **2002**, *413*, 186.